Bulletin of the New Zealand Society for Earthquake Engineering, Vol. 58, No. 2, June 2025

ASSESSING THE LIFE-SAFETY RISK FOR THE PROPOSED TECHNICAL SPECIFICATION (TS) 1170.5

Anne M. Hulsey[1], Kenneth J. Elwood[2], Nick Horspool[3], Matthew C. Gerstenberger[4] and Timothy J. Sullivan[5]

(Submitted *April 2024*; Reviewed *June 2024*; Accepted *March 2025*)

ABSTRACT

The current New Zealand seismic design provisions are expected to be updated with a proposed Technical Specification (TS). The update is motivated primarily by the recent release of the 2022 National Seismic Hazard Model, with new seismic hazard estimates across the country. The updates are being carried out by the Seismic Risk Working Group (SRWG). One of the SRWG's primary intentions for the proposed TS was to maintain the Building Code objective of safeguarding people from injury in light of these hazard changes. While previous code development in New Zealand has not explicitly assessed whether the life-safety risk was tolerably low, the SRWG sought to implement a new life-safety risk assessment methodology. The risk assessment takes an Ultimate Limit State (ULS) design spectrum as input and provides an expected distribution of the fatality risk, representing the variety of buildings that could be designed in accordance with the minimum requirements associated with ULS. The methodology is made up of four modules representing (A) the shaking hazard, (B) the building performance (collapse fragility), (C) the probability of fatality given collapse, and (D) the variability in performance among code-conforming buildings. The first three modules quantify fatality risk for a single building, while the fourth module iterates over many buildings to produce a full risk distribution. Using this methodology, the SRWG found that for Importance Level 2 (IL2) buildings, a ULS design spectrum with an annual probability of exceedance ($APoE$) of 1/500 typically corresponds to an annual individual fatality risk ($AIFR$) ranging between 10^{-6} and 10^{-5}. Comparison with the ULS design spectra from the current NZS 1170.5:2004 provisions shows that the proposed spectra result in more uniform risk across the country, across different site classes, and across different periods. Additionally, the IL3 ULS design spectrum with an $APoE$ of 1/1000 was considered, demonstrating that increasing the importance level to mitigate mass casualty events in high occupancy buildings is functionally equivalent to reducing the tolerable $AIFR$ level. In summary, the risk assessment methodology can provide valuable information to the code development process by evaluating and comparing the life-safety risk associated with various options for the ULS design spectra.

https://doi.org/10.5459/bnzsee.1690

INTRODUCTION

The recent release of the 2022 National Seismic Hazard Model (NSHM) [1] has prompted re-examination of the New Zealand seismic design provisions, NZS 1170.5 [2]. In response, the Ministry for Business, Innovation, and Employment (MBIE) asked Engineering New Zealand (ENZ) to form the Seismic Risk Work Group (SRWG) to propose updates to the primary verification method for the New Zealand Building Code (B1/VM1) [3]. This multi-year project seeks to develop improvements to New Zealand seismic design practice, most notably updates to NZS 1170.5. The first stage of the project drafted a proposed Technical Specification document, TS 1170.5, offering an alternative methodology to determine seismic design loads for buildings. This paper reflects the latest changes (as of the publication date) to the draft document, which is expected to be published in 2025 and is hereby referred to as the "proposed TS" or simply, TS.

The TS incorporates the latest NSHM into acceleration spectra for use in design, $S_a(T)$, as described in companion papers [4,5]. This paper provides an assessment of how well the proposed spectra satisfy the performance objectives of the NZ Building Code [6]. In particular, it focuses on how the ultimate limit state (ULS) provisions address the first objective, B1.1 (a) "Safeguard people from injury caused by structural failure." The building performance associated with achieving this objective is defined in B1.3.1 as "a low probability of rupturing, becoming unstable, losing equilibrium, or collapsing" [6]. By assessing the fatality risk associated with designing for the ULS spectra, the SRWG was able to evaluate whether the results were consistent with the intent of these clauses.

It is worth noting that the SWRG's framework for assessing risk differs from the widely recognized "risk-targeted" framework, which sets the design spectra by explicitly targeting a risk value. In the United States, this is a risk of building collapse [7], while other studies consider fatality risk [8,9]. However, as described over the course of this paper, the SRWG preferred to (1) allow other drivers to influence the ULS design spectra, in addition to risk and (2) consider the full distribution of risk across a variety of buildings, not just a single, average value of risk.

Ultimate Limit State

The design spectra associated with ULS can be found in the Site Demand Parameter Tables in the TS, by referencing the relevant

[1] *Corresponding Author, Research Fellow, University of Auckland, Auckland, anne.hulsey@auckland.ac.nz, (Member)*
[2] *Chief Engineer, Ministry of Business, Innovation and Employment (MBIE) / Earthquake Commission (EQC), Wellington, (Fellow)*
[3] *Risk Specialist, GNS Science, Lower Hutt, (Member)*
[4] *Seismologist, GNS Science, Lower Hutt, (Member)*
[5] *Professor, University of Canterbury, Christchurch, (Member)*

annual probability of exceedance ($APoE$), location, and site class. This paper focuses on importance level 2 ($IL2$) buildings so the ULS $APoE$ is 1/500, as specified in AS/NZS 1170.0 [10]. A later section will also consider $IL3$ buildings. The example locations in this paper include Wellington, Auckland, Christchurch, and Dunedin, as well as several others. While all the TS site classes were evaluated, the baseline results consider Site Class IV, which is one of the site classes commonly found in populated regions across New Zealand. Though there is no one-to-one relationship between the NZS 1170.5:2004 and TS site classes to serve as a reference, the closest NZS equivalent is Site Class D.

The proposed $S_a(T)$ design spectra typically represent the mean NSHM for a given $APoE$, based on the representative $V_{s(30)}$ value for which the site class spectrum was derived (e.g., $V_{s(30)} = 275$ *m/s* for Site Class IV) [5]. However, this paper will demonstrate cases in which the proposed $S_a(T)$ spectra do not strictly match the underlying NSHM spectra for the location, due, for example, to the fitted $S_a(T)$ shape or a different $V_{s(30)}$. One of the most significant differences between the proposed spectra and the mean NSHM occurs in Auckland and Northland. Rather than being based on the mean, these locations are controlled by the TS's lower bound hazard, defined as Auckland's 90^{th} percentile spectrum [3]. (See Module A for the distinction between the mean and percentile hazards.). This paper will demonstrate how the differences between the $S_a(T)$ used in design relative to the site's mean NSHM hazard can influence the risk assessments.

Tolerable Risk

The purpose of the risk framework is to evaluate whether the proposed $S_a(T)$ design spectra result in tolerable risk levels, using the risk assessment methodology. As noted previously, the NZ Building Code calls for "safeguard[ing] people from injury caused by structural failure" by ensuring a "low probability" of behaviours like collapse that may result in both fatal and non-fatal injuries. The question, then, is what qualifies as a tolerably low probability.

The tolerability of risk is often represented as two bounds, a lower bound marking what is clearly unacceptable and an upper bound for clearly acceptable, with a large range of tolerability in between [11]. Within this range, the tolerance depends on many factors, including perceptions around the cost of achieving a reduced risk and the associated benefits. One such factor is the preference for codified verification methods in national seismic loading standards, which inherently produce a range of risk levels among code-conforming buildings, as opposed to a more onerous design process that could evaluate and design individual buildings for a specific risk target. Due to the influence of these multiple factors, the SRWG chose to first develop $S_a(T)$ spectra for ULS design, then use the risk assessment methodology, described herein, to check whether the risk would be deemed tolerable.

One commonly used metric for life-safety is the probability that an individual in a given location (in this case a building) is killed in an incident (in this case an earthquake), termed here as the annual individual fatality risk, $AIFR$ [12]. Yet there are no universally agreed upon $AIFR$ values for the clearly acceptable and unacceptable bounds. More specifically in New Zealand, there is no regulatory framework setting out fatality risk tolerance [11]. However, various sectors and authorities in New Zealand have developed a number of risk tolerability guidelines that can be compared. These guidelines are mostly for land-use planning and have been developed by Christchurch City Council, Otago Regional Council, Bay of Plenty Regional Council and Whakatane District Council [11]. The tolerable range of $AIFR$ from these sources typically varies by an order of magnitude, with an upper limit (beyond which the risk is unacceptable) of 10^{-5} or 10^{-4}, depending on the study. A literature review [13] compared international risk criteria from the United Kingdom, the Netherlands, Australia, Hong Kong, and Iceland. They also include upper limits up to 10^{-4}, while some are as low as 10^{-6}. Similarly, ISO 2394, General Principles on Reliability for Structures [14], provides international examples with tolerable upper bounds ranging from 10^{-6} to 10^{-5}.

As can be seen, there is considerable variability in $AIFR$ values selected as the upper limit of tolerability. Rather than select one definitive value from among the available precedents, the SRWG preferred to conceptualize the risk tolerability as a range. This is consistent with the recognition that code-conforming buildings will have a wide range of risk outcomes. While "risk-targeted" methods for setting design spectra [7–9,15] implicitly acknowledge this variability, they are sometimes misconstrued as an expectation of achieving the specific risk target value for each building. By considering a distribution of risk, the SRWG approach is considered to be more transparent, both in communication and in being able to consider the distribution of risk values across all potential new buildings, not just the average risk.

The risk tolerability range was deemed to be roughly 10^{-6} to 10^{-5}, based on the references above, as well as other constraints such as the aforementioned perceptions of costs and benefits. The range's blurred bounds are depicted in Figure 1. The risk distribution within the tolerable band should be dominated by lower risk values, such that having most of the distribution fall just below 10^{-5} would not be considered tolerable. However, recognizing the blurred nature of the range and the order-of-magnitude level of crudeness for the bounds, it is also tolerable to have some small portion of the risk distribution fall above 10^{-5}. Likewise if a large portion of the risk falls well below 10^{-6}, this would suggest that the design settings may be too risk averse, resulting in higher costs of construction than necessary. The metrics used in this paper for visually comparing the risk distribution to the tolerable range are the 50^{th} percentile (median), mean, and 90^{th} percentile. As will be demonstrated in the subsequent results, the mean and median should fall within the risk tolerability range, while the 90^{th} percentile is ideally no more than $2x10^{-5}$ (2x the upper bound).

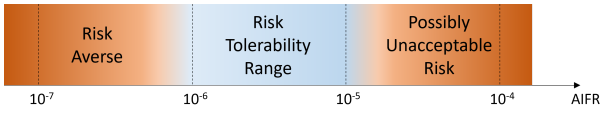

Figure 1: Risk tolerability range for annual individual fatality risk in code-conforming buildings.

RISK ASSESSMENT METHODOLOGY

The SRWG's risk assessment approach starts with developing a potential definition of ULS spectra, such as a given $APoE$ level, then assessing the associated risk to evaluate whether the outcome is tolerable. This approach can be termed "risk-informed," as risk is considered in establishing the ULS design spectra but is not an initiating driver. This flow is consistent with the lack of a single risk value to "target" for all buildings. In addition to considering the absolute values of risk, another goal of the risk-informed approach is to achieve more uniform risk levels across the country, as well as across periods and site classes. Once again, it is recognized that there will never be equal risk but the methodology can assess whether the variability

in risk is tolerable, as well as explore comparisons with the risk provided by NZS1170.5:2004 *ULS* design spectra.

The centre of the framework is the risk assessment methodology, which is based on well-established risk concepts [16]. The framework's conceptual extension is that it produces a risk distribution rather than a single value. The assessment tests the tabulated $S_a(T)$ design spectra to see whether the resulting distribution of risk is tolerable, as depicted in Figure 2. The assessment starts by quantifying the shaking hazard (Module A) as the probability of exceeding a given shaking intensity for a range of increasing intensity levels (i.e., hazard curves, Figure 3). The shaking hazard is paired with a probabilistic representation of building performance (Module B), where the probability of collapse increases with the shaking intensity (i.e., a collapse fragility curve, Figure 4). Combining the shaking hazard with the building performance in a risk integral calculates the total risk of building collapse over the full range of shaking intensities (Figure 5). Including the probability of fatality given collapse (Module C) produces a single value of fatality risk. However, in reality, any number of buildings could be designed in compliance with the TS minimum requirements, yet may exhibit very different building performance, depending on the structural system, the presence of irregularities, or a range of other design choices. Therefore, this variability among buildings (Module D) is introduced by randomly sampling the building performance (B) to get a likely distribution of risk.

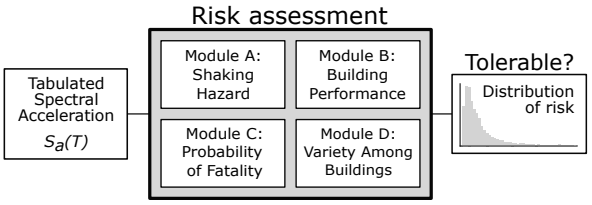

Figure 2: Conceptual framework for evaluating the risk tolerability associated with the TS tabulated spectral acceleration, $S_a(T)$.

The process described above is formally defined in Equation 1, for the annual individual fatality risk, $AIFR$. The shaking hazard, $P(IM > im)$, is the probability of exceeding the intensity, im. The building performance is included in the second term, the derivative of the collapse fragility at the intensity, $P(C|im)$. The final term is the probability of fatality given collapse, $P(F|C)$. The terms in the risk integral represent the models discussed in more detail below, with a summary provided in Table 1.

$$AIFR = \int_0^\infty P(IM > im) \times \frac{d(P(C|im))}{d(im)} d(im) \times P(F|C) \quad (1)$$

Shaking Hazard (Module A)

Shaking hazard refers to the likelihood of a given level of earthquake shaking for a particular location, soil stiffness, and fundamental period. The shaking hazard used in the risk assessment represents the probability of shaking across all levels of intensities. This is different from the discrete hazard values associated with various design limit states at specific *APoE* levels. Rather, it is a hazard curve, covering a full range of intensities to quantify the probabilities of exceeding each. Using a hazard curve to assess risk captures the impact of all intensities, including the potentially high influence of intensities beyond the design limit states. This is particularly important for life-safety risk assessments, as most of the risk is accumulated at intensities beyond that of *ULS* design.

The hazard curves quantify the probability of exceeding a given shaking intensity, as demonstrated in Figure 3a with three hazard curves. The y-axis shows the probabilities of exceedance, with reference lines marking the *APoE*s of 1/500, 1/2500, and 1/10,000. The level of shaking is characterized by an intensity measure, *IM*, on the x-axis. The *IM* is defined here as the pseudo-spectral acceleration, $Sa(T)$, shown in Figure 3a for the fundamental periods $T = 0.5$, 1, and 3 seconds (green, orange and blue, respectively). These hazard curves can be found on the NSHM web portal (nshm.gns.cri.nz), which provides the hazard for all sites across the country, considering a range of soil stiffnesses (characterized by the average shear wave velocity over the top 30 meters, $V_{s(30)}$), and fundamental periods ranging from $0 \leq T \leq 10$ seconds. The hazard curves in Figure 3a are for Wellington with $V_{s(30)} = 275$ *m/s*. This $V_{s(30)}$ value was selected as representative of Site Class IV, noted previously as a typical site class across New Zealand cities.

The NSHM considers epistemic uncertainty in the rupture source models (the location and rate of various types of tectonic events) and the ground motion models (the intensity of the ground shaking due to those events) [1]. This reflects the fact that, while there is theoretically a "true" hazard that could be identified with perfect data, the existing data can only provide a distribution of possible hazard curves that includes the true (yet unknown) hazard. As a result, the NSHM is made up of a suite of hazard curves that can be characterised by a distribution at each APoE level. The NSHM web portal provides the mean and percentile *IM* values of these distributions, where the x^{th} percentile represents x% confidence that the hazard is below $IM_{x^{th}}$. The median (50^{th} percentile) and mean are both central estimates of the distribution. The median provides a 50-50% confidence that the hazard is above or below $IM_{50^{th}}$, while the mean also reflects the shape of the distribution, such as being skewed to one side. The mean was selected as the defining hazard metric for all the SRWG life-safety risk assessments presented in this paper.

The slope of the hazard curve is a significant driver of the risk.

Table 1: Description of each module in the risk assessment methodology.

	Module	Features
A	*Shaking Hazard*	- probability of exceedance over a range of shaking intensities - mean hazard from NSHM for location, $V_{s(30)}$, and period
B	*Building Performance*	- collapse fragility linked to *ULS* through the collapse margin ratio, *CMR* - shape defined by a lognormal distribution with *CMR* as the median and β as the lognormal standard deviation
C	*Probability of Fatality*	- fatalities are conditioned on the event of collapse - probability of fatality given collapse = 10%
D	*Variety among Buildings*	- distribution of fragilities to represent variability among buildings - *CMR* ranging from 3 to 9, βs ranging from 0.35 to 0.45

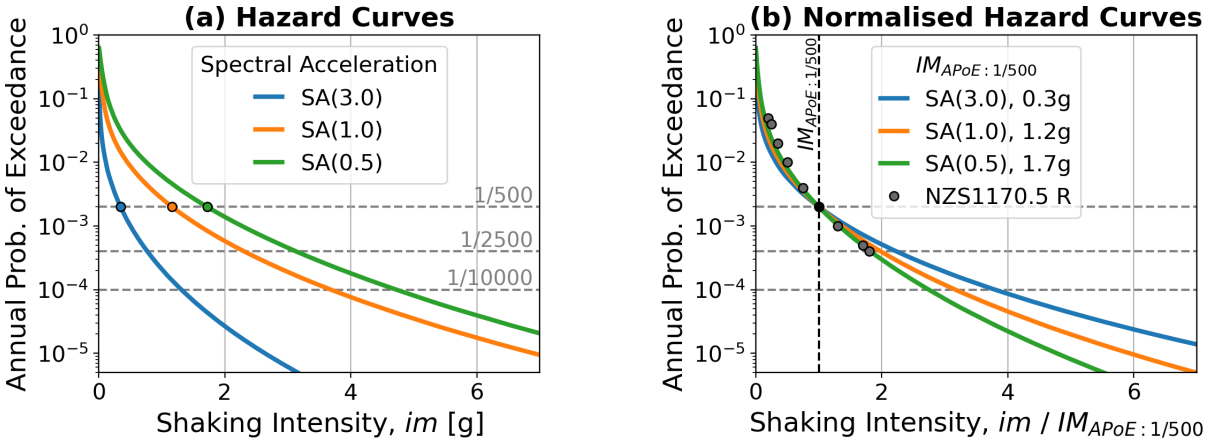

Figure 3: Quantifying the shaking hazard. (a) Wellington, $V_{s(30)} = 275$ m/s (Site Class IV) spectral acceleration hazard curves for fundamental periods, T = 3, 1, and 0.5 seconds (blue, orange, green, respectively). The circle markers denote the shaking intensity with a 1/500 annual probability of exceedance, $IM_{APoE:1/500}$. (b) The same hazard curves as in (3a), normalised by the $IM_{APoE:1/500}$ values listed in the legend. The NZS1170.5:2004 return period factors, R, are included for reference (gray circles).

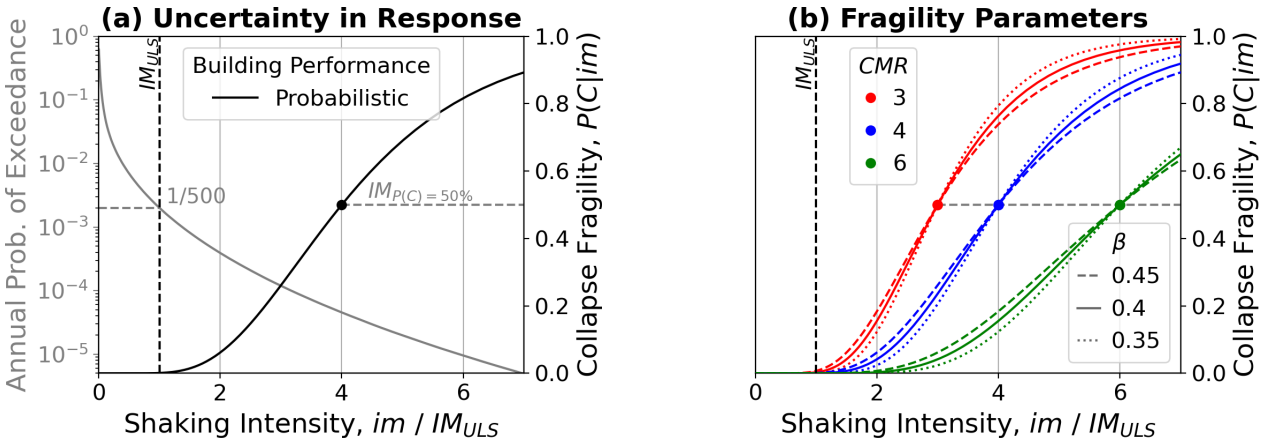

Figure 4: Quantifying the building performance as the probability of collapse over increasing shaking intensities, $P(C|im)$. (a) Probabilistic building performance in the form of a collapse fragility: The circle marker at $IM_{P(C)=50\%}$ is the median collapse intensity, while the shape is defined by the cumulative density function of a lognormal distribution. The shaking intensity for the ultimate limit state, IM_{ULS}, is taken as the 1/500 annual probability of exceedance of the grey hazard curve. (b) Estimating the collapse fragility: The median collapse intensities are defined by the collapse margin ratio (CMR), as a multiple of the IM_{ULS} (red, blue, green circle markers show CMR = 3, 4, 6, respectively). The slope of the fragilities are defined by β, the lognormal standard deviation (dotted, solid, and dashed lines show β = 0.35, 0.4, and 0.45, respectively).

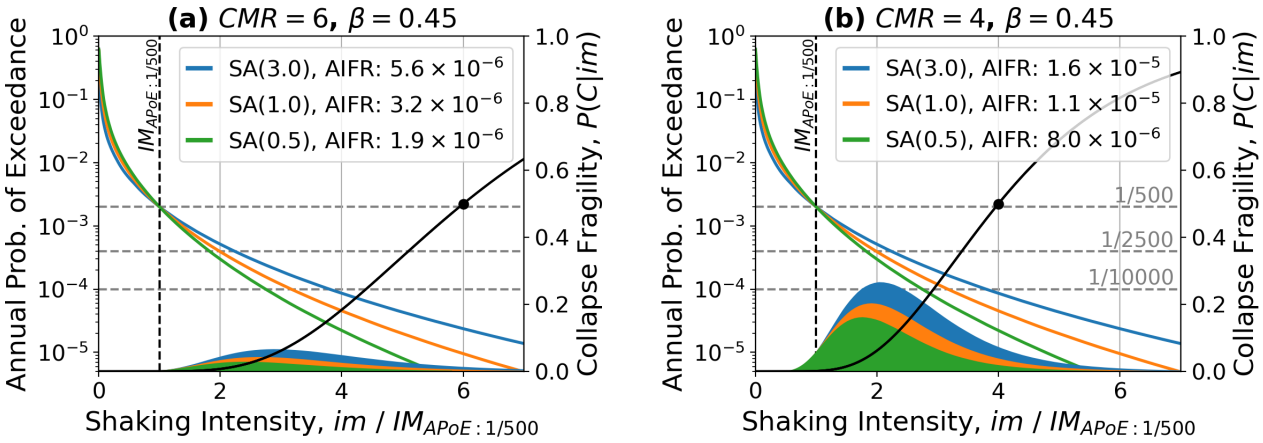

Figure 5: Quantifying risk as the convolution of a hazard curve (Figure 3b) and a collapse fragility (Figure 4). The top edge of the colored shapes (fundamental periods of T = 3, 1, and 0.5 seconds as blue, orange, and green, respectively) is the integrand in Eqn. 1, with the area under the curve noted in the legend as the annual individual fatality risk, AIFR. (a) A collapse fragility with a collapse margin ratio (CMR) of 6 and a lognormal standard deviation (β) of 0.45. (b) A collapse fragility with CMR = 4 and β = 0.45.

While the steepness of each curve in Figure 3a can be inferred by the increase in *im* between the reference *APoE* lines, they can be more easily compared by normalising each curve by its respective *APoE* of 1/500 value, $IM_{APoE:1/500}$, as in Figure 3b. The *APoE* of 1/500 was chosen as the reference value for this figure because the normalised x-axis provides a direct comparison to the return period factor, R, in NZS 1170.5:2004 Table 3.5 and shown as gray circles in Figure 3b. For example, the three curves cross the horizontal *APoE* of 1/2500 line at 1.8, 2.0 and 2.2, for $T = 0.5$, 1 and 3 seconds, respectively. While these are relatively similar to the single $R = 1.8$ value used in NZS1170.5:2004, the variability across periods does influence the fatality risk, as discussed in Module C with respect to Figure 5.

Building Performance (Module B)

The building performance module uses fragility functions to quantify a building's probability of exceeding a limit state (*LS*) over a range of *IM* values, $P(LS|im)$. The choice of *IM* is linked to the hazard curve and serves as a proxy for the seismic demands experienced by the building. This means that two ground motion records that are characterized by the same *IM* value, *im*, may have very different acceleration time histories (e.g., with different spectral shapes or a long versus short duration). This abstraction from the time history to the *IM* introduces record-to-record variability, RTR, in the *im* at which the building will exceed the limit state. This and other sources of uncertainty are quantified as a fragility function (Figure 4a), centered around the median $IM_{P(LS)=50\%}$, or the intensity at which the building has a 50% chance of exceeding the *LS*.

While the design criterion for life-safety is based on *ULS*, the fatality-risk assessment is based on the collapse limit state, *CLS*. The collapse limit state is preferred because fatalities are more closely linked to the probability of collapse as described below in Module C. Figure 4a shows a collapse fragility normalised by the *ULS* intensity, IM_{ULS}. (A hazard curve is also included in gray, showing a IM_{ULS} that corresponds to an *APoE* of 1/500.) Normalising the collapse fragility redefines the median collapse intensity (also known as the collapse capacity), as a collapse margin ratio, $CMR = IM_{P(C)=50\%}/IM_{ULS}$. The black circle marker in Figure 4a represents a *CMR* of 4. Defining the median as a *CMR* based on *ULS* provides a simple link between the design limit state and the building collapse performance. (Note that this definition does not specify any values of *CMR*, which will be discussed in Module D.)

Defining the collapse capacity as the *median* collapse intensity implies that there is uncertainty in the actual intensity at which the building will collapse. This uncertainty is quantified by the shape of the fragility curve that passes through the median. The shape is conventionally characterized by the cumulative distribution function of a lognormal distribution with a median (defined here as *CMR*) and a lognormal standard deviation of β (e.g. [17]). Small βs produce a relatively steep fragility curve, suggesting that collapse will likely occur at an intensity close to the median, while larger βs flatten the fragility curve to denote increased uncertainty in the collapse intensity. The fragility curve also flattens as the *CMR* increases, since the uncertainty in the collapse intensity is proportional to the median. These effects of *CMR* and β on the resulting collapse fragilities can be seen in Figure 4b.

Part of the uncertainty in the collapse intensity, as already noted, accounts for the record-to-record variability, β_{RTR}. Some *IM*s serve as better proxies for the seismic demands than others, reducing β_{RTR}. For example, instead of using the spectral acceleration at a building's fundamental period, $Sa(T)$, the average spectral acceleration, Sa_{avg}, can be calculated over a range of periods (e.g., $0.2T < T_i < 3T$) [18]. The spectral shape of an acceleration time history is often characterized by $SaRatio = Sa(T)/Sa_{avg}$ [19]. Alternatively, vector *IM*s use multiple dimensions to describe the ground motion intensity, such as in the site-specific adjustment framework for incremental dynamic analysis (SAF-IDA) [20]. SAF-IDA considers a building fragility's sensitivity to the correlation between $Sa(T)$, *SaRatio*, and significant duration (D_{S5-75}) by disaggregating the site hazard at each intensity level of interest, IM_{APoE} [21]. However, even improved *IM*s are only a proxy for the seismic demands imposed on a building by a unique acceleration time history. Therefore, the SRWG risk assessments take the simpler approach of using $Sa(T)$, thereby maintaining consistency with both the TS tabulated $S_a(T)$ design spectra for *ULS* and the shaking hazard provided by the NSHM. The use of $Sa(T)$ is also consistent with international best practice (e.g., [17,22]).

Another source of uncertainty is in the collapse capacity itself, *CMR*. This uncertainty is due both to the variability among buildings, each with their own capacity, and to the uncertainty associated with material properties and modeling methods for quantifying the performance of each building. For example, the FEMA P695 methodology used in the United States to assess the collapse risk of new structural systems accounts for uncertainty in design requirements, test data, and modeling [17]. The total β is taken as the combination of each source of uncertainty. This approach provides an average, flattened fragility (higher β) that conceptually represents the mean of a distribution of fragilities [23]. The risk-targeted framework tends to use this approach, with β values between 0.5 and 0.8 [7–9,15]. The SRWG risk assessment, on the other hand, is interested in the distribution of risk associated the full distribution of possible fragilities, not just a single, average fragility. Module D will discuss a distribution of collapse capacities among individual buildings, i.e., the *CMR* values used in the risk assessment. Explicitly including the uncertainty in the collapse capacity in this way means that the individual fragilities need only include the RTR portion of β. Most buildings that experience period elongation (i.e., exhibit a ductile response that softens the initial stiffness) have $0.35 \leq \beta_{\text{RTR}} \leq 0.45$ for collapse fragilities based on $Sa(T)$ [17]. The method of combining *CMR*s and β for a distribution of fragilities is discussed in more detail in Module D.

Probability of Fatality (Module C)

As previously stated, in the siesmic design context, the annual individual fatality risk, *AIFR*, is the probability that an individual in a given building is killed in an earthquake. The majority of building-related deaths and serious injuries in recent New Zealand and international earthquakes have been caused by partial or complete structural collapse [24,25]. The *AIFR*, therefore, can be reformulated as the probability that an individual is killed in a collapse, conditioned on the given building's probability of collapse, as calculated by the first and second terms in Equation 1 (Modules A and B). While the *AIFR* applies this probability of fatality to a single individual located in the building, it is also applicable in estimating the number of fatalities as a percentage of the total number of occupants. In fact, estimates for the probability of fatality are often based on the percentage of occupants killed.

The probability of fatality given that the building has collapsed, $P(F|C)$, will depend on the collapse mode, structural system, and other factors. One way to account for this variability in building response is to consider an event tree of collapse modes, C_{mode_i},

with a unique probability of fatality for each event, $P(F|C_{mode_i})$ [26]. Using Bayes' Theorem, a building's total probability of fatality given collapse, $P(F|C)$, can be derived from this event tree, using the probability of each collapse mode given collapse, $P(C_{mode_i}|C)$ [27]. While the resulting $P(F|C)$ is an expected value (i.e., does not explicitly account for the range of potential number of fatalities given collapse), the variability is implicitly accounted for through the event tree.

While the event tree described above is conceptually simple, it is difficult to assign either the $P(F|C_{mode_i})$ or $P(C_{mode_i}|C)$ probabilities for a given building. This is a form of epistemic uncertainty, whereby the selected model of building performance is one of many possible event trees. When considering $P(F|C)$ for a building code-level risk assessment, there is also the inherent randomness (aleatory variability) associated with variations among potential code-conforming buildings. While the variability among buildings could also be introduced as branches in the event tree, it is simpler to use engineering judgment to assign a single $P(F|C)$ as the expected value. HAZUS, a commonly used tool for regional loss estimation, assigns a 15% probability of fatality for most structural types (10% immediate loss of life + 5% life-threatening injuries), with additional nuance for partial collapses that would not affect the entire building population [28]. A more recent study compiled fatality ranges from existing literature and suggested building class-specific $P(F|C)$ values for use in the US Geological Survey's semi-empirical loss estimation model [29]. The suggested $P(F|C)$s for reinforced concrete (RC) and steel structural systems range between 5 to 12% for 1- to 3-storey buildings, 8 to 25% for 4- to 7-storey buildings, and 15 to 40 % for 7+ storey buildings. The upper bounds of these ranges represent RC frames, with over 2× the suggested $P(F|C)$ values as compared to RC shear walls and steel frames. For catastrophic collapse modes, the suggested values range between 40 and 80%, depending on the height of the building. These values for catastrophic collapse are partially based on data from the Christchurch earthquake, where the two significant building collapses were in pre-2004 buildings not in compliance with modern codes [29]. Given the low probability of catastrophic collapse modes in new seismically engineered structures, as well as the prevalence of shorter buildings, the TS risk assessments use an expected value of $P(F|C) = 10\%$, as is done in other risk-targeted studies (e.g. [8,9]). The results would scale linearly for alternate $P(F|C)$ values.

Modules A through C correspond to each of the three terms in the risk integral, Equation 1. The concept is shown visually in Figure 5. The blue, orange, and green hazard curves in both subfigures are identical to those in Figure 3b for $T = 3$, 1, and 0.5 seconds. The circles on each black fragility curve mark *CMR*s of 6 and 4 in Figures 5a and b, respectively, with $\beta = 0.45$ for each. In each figure, the integrand is computed for each hazard curve with the fragility curve and is shown as the corresponding shaded shape lying on the x-axis. The total shaded area below the integrand is the fatality risk, labeled as *AIFR* in the legend. The shape of the integrand, known as the risk disaggregation, portrays the relative contribution of each *im* to the total fatality risk.

In each figure, the risk is highest for $T = 3$ seconds, due to the relative shapes of the normalised hazard curves beyond $IM_{APoE:1/500}$. It is typical for longer periods to have relatively higher intensities for *APoE*s less than 1/500. The risk integral captures the impact of this type of variability in the hazard curve, which changes with period, $V_{s(30)}$, and location. However, the difference between two buildings' collapse capacities can have an even greater effect than the variability in the shape of the hazard curve, as seen by comparing the risk for the *CMR* = 4 and 6 values in the left and the right figures, respectively. This variability in collapse capacities is discussed next.

Variability Among Buildings (Module D)

The risk assessment methodology explicitly considers variability in collapse performance among buildings, due to both design decisions and the uncertainty in actual performance for a given design. As discussed in Module B, this variability is often addressed implicitly by using a single, average collapse fragility with relatively high uncertainty (β) to represent an underlying suite of many fragilities. Instead, the SRWG risk assessment produces a risk distribution by iteratively re-calculating the risk integral over a suite of likely collapse fragilities. The suite of fragilities is developed based on underlying distributions of the two defining parameters, *CMR* and β.

The distribution of *CMR*s has a more significant effect on the risk distribution than β, as the *CMR* distribution represents a wide range of potential collapse capacities among building designs that conform to the minimum requirements. Through consultation with the SRWG and review of existing literature, a range of $3 \leq CMR \leq 9$ was selected to represent the variability among New Zealand's modern, code-compliant buildings. The lower bound is consistent with analytical studies suggesting that new code-compliant buildings are likely to sustain earthquake shaking levels ranging from 3 to 5 times the *ULS* design spectra prior to collapse [30–32]. The upper bound reflects the fact that other decisions (beyond the minimum design requirements) may improve the performance, as well as the notion that experimental and analytical research studies may provide conservative estimates of collapse performance, as compared to field observations. This conservatism is due to a variety of factors, including conservative definitions of collapse (e.g. 5% peak storey drift), the presence of (unmodeled) gravity-load resisting systems that improve performance, and the effects of soil-structure-interaction (which are beneficial in the majority of cases), among others. The largest values of *CMR* would represent buildings where seismic loads were not found to be critical and/or where the inherent ductility and deformation capacity are underestimated by current material standards. While the 3 to 9 range defines the minimum and maximum, the SRWG risk assessment methodology needs a distribution, describing how frequently each *CMR* is expected amongst a population of new buildings. The SRWG's selected distribution of *CMR* values is characterized as a truncated normal distribution, with a mean of 6 and a standard deviation of 1.5, and resampling for any values below the minimum of 3 or above the maximum of 9. This shape means that *CMR* values of 3 and 9 are less common than intermediate values. This can be seen conceptually in Figure 6a, where the gray histogram represents 100 *CMR* values sampled from the underlying distribution.

The distribution of βs represents the uncertainty in each individual building's collapse *im*. As discussed previously, this is limited to β_{RTR}, with the other typical sources of uncertainty being included in the *CMR* distribution. The distribution of βs is characterized as a uniform distribution between $0.35 \leq \beta \leq 0.45$, consistent with the typical β_{RTR} range for buildings that experience period elongtation [17]. Once again, this is shown in Figure 6b with a gray histogram representing 100 sampled β values. The sampled *CMR* and β values are randomly paired together to create the sampled fragilities in Figure 6c.

The sampled fragilities are a representation of the underlying *CMR* and β distributions. No two sets of sampled fragilities will be exactly the same. However, the effect of this variability on the risk distribution can be reduced by increasing the number of samples. The results discussed in the next section are based

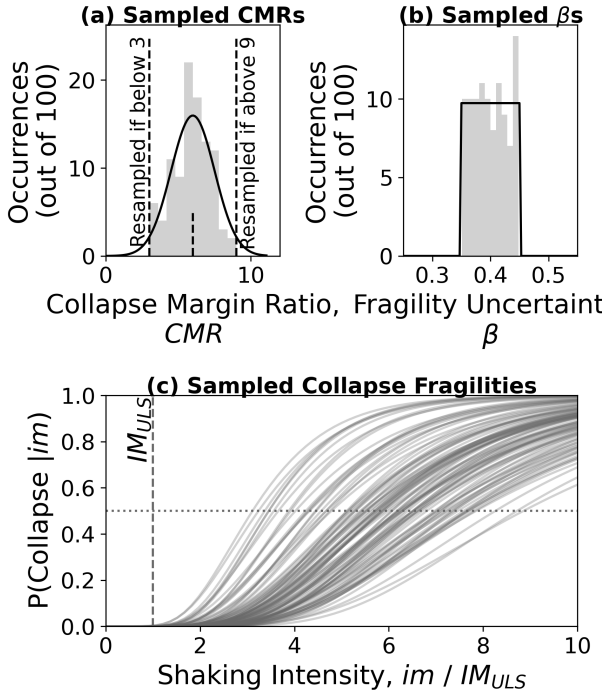

Figure 6: Accounting for variability among buildings (Module D): (a) a histogram of sampled collapse margin ratios (CMRs) using a normal distribution with a mean of 6 and a standard deviation of 1.5 and resampling below 3 and above 9. (b) a histogram of sampled β values, using a uniform distribution between 0.35 and 0.45. (c) Sampled fragility curves, given the CMR and β values from (a) and (b). The fragilities are normalised by the ULS intensity, IM_{ULS}, at the dashed vertical line. Each fragility crosses the horizontal dotted line for P(Collapse\|im)=50% at its CMR value.

on 5000 sampled fragilities. In some of the studies below, the general trends were studied by use of a single fragility, rather than the suite of fragilities for a full distribution. A fragility with $CMR = 6$ and $\beta = 0.45$ is selected for this purpose, as it is conceptually similar to the "average" fragility used in FEMA P695. While this approach is not formally consistent with the SRWG risk assessment methodology, the resulting risk value typically falls between the median and mean of the full risk distribution.

This concludes the description of the modules. Further nuances of the risk assessment methodology will be introduced in the next section as the process is demonstrated and the results discussed.

ASSESSING THE LIFE-SAFETY RISK DISTRIBUTION

The life-safety risk assessment considers whether the $S_a(T)$ spectra for ULS design of $IL2$ buildings are consistent with the building code objective, based on the resulting distribution of fatality risk. Other than historical and international precedent, there appears to be no formal justification for the $APoE$ of 1/500 defined for ULS. Thus, this methodology provides a mechanism to confirm whether the fatality risk associated with the ULS definition is tolerable and appropriate for new construction in New Zealand. The results will be explored below, starting with Wellington.

Wellington

The introductory discussion of each module already included some results for Wellington with $V_{s(30)} = 275$ *m/s*, as a way of understanding the risk integral. Figure 5 showed the fatality risk, $AIFR$, for three different periods, depending on the collapse fragility used in each subfigure ($CMR = 6$ or 4). The purpose of the figure was conceptual, rather than a formal assessment of the tabulated TS $S_a(T)$ spectra. As such, it was assumed that $IM_{ULS} = IM_{APoE:1/500}$ for all periods. However, as can be seen in Figure 7a, there is a slight variation between the underlying shaking hazard's uniform hazard spectrum (UHS) for an $APoE$ of 1/500, as provided by the NSHM (dashed line), versus the TS design spectrum $S_a(T)$ for ULS (solid line). This difference is most apparent in Figure 7b, showing the ratio between the two, $ULS/UHS_{APoE:1/500}$. The effect of this difference is to shift the hazard curve slightly with respect to the fragility, as the fragility's CMR is normalised by the ULS value rather than the hazard curve's $UHS_{APoE:1/500}$. If $ULS > UHS_{APoE:1/500}$, the code minimum is slightly conservative with respect to the mean hazard curve, resulting in lower fatality risk. For the Wellington spectra shown in Figure 7b, the difference between ULS and $UHS_{APoE:1/500}$ is minimal and incidental, due only to the functional form of the TS spectral shape. As will be shown later, the difference for the Auckland spectra is intentional, as implemented by the lower bound hazard.

The risk assessment methodology produces a distribution as seen by the gray histograms in Figure 8, showing the fatality risk for Wellington's ULS for Site Class IV. The shaking hazard is evaluated for the site class's representative value, $V_{s(30)} = 275$ *m/s*. For $T = 0.5$ seconds, in Figure 8a, the distribution dominates the far left of the figure, with the 90^{th} percentile (triangle marker) near $0.5x10^{-5}$ $AIFR$. The 50^{th} percentile (diamond) and mean (circle) are near $0.2x10^{-5}$ $AIFR$. For $T = 1$ seconds, the whole distribution is shifted right, while the distribution for $T = 3$ seconds is higher still. These shifts are due to the difference in the shape of the hazard curves for increasing periods from 0.5 to 3 seconds. If the SRWG's primary goal for ULS design were uniform risk across all periods, a risk factor could be introduced to decrease the $S_a(T)$ spectrum at short periods and increase it at long periods. However, it was decided that such a complexity was not justified at this time.

Similar trends can be observed in Figure 9 for all site classes (I - VI) and four periods ($T = 0.5$, 1, 1.5, and 3 seconds). In this figure, each vertical line corresponds to one histogram as shown in Figure 8, with the white markers denoting the same summary metrics. Once again, the risk for each site class grouping is evaluated for the representative $V_{s(30)}$ hazard curve. This vertical orientation futher highlights the increasing risk with respect to period that Figure 8 demonstrated for Site Class IV. This trend is also present for other site classes, though it may be modified by the variability in the $IM_{ULS}/IM_{APoE:1/500}$ ratio, as can be seen by comparing the results for site classes III - V with the ratios in Figure 7b. (See Figure 15 for further explorations of deviations from this trend.) As noted before, the SRWG determined that the benefit of reducing the period-based variability did not warrant the additional complexity of including a risk factor, particularly given that the mean risk is well within the risk tolerability range and the 90^{th} percentiles are no more than $2x10^{-5}$.

Another dimension to consider is the soil stiffness, which informs the site class. In Figure 9, all six site classes are displayed, with the risk evaluated at each class's representative $V_{s(30)}$ value. This is the $V_{s(30)}$ value at which each site class's tabulated $S_a(T)$ spectra were derived from the underlying NSHM [5]. However, a Site Class IV may be assigned to sites with $V_{s(30)}$ values ranging from 250 to 300 *m/s*. Or, more dramatically, a site assigned a Site Class II could have a $V_{s(30)}$ as low as 450 or as high as 750 *m/s*. Because buildings designed for a single site class will have variable hazard exposure depending on the underlying $V_{s(30)}$ value, their risk will also vary. The impact of this hazard

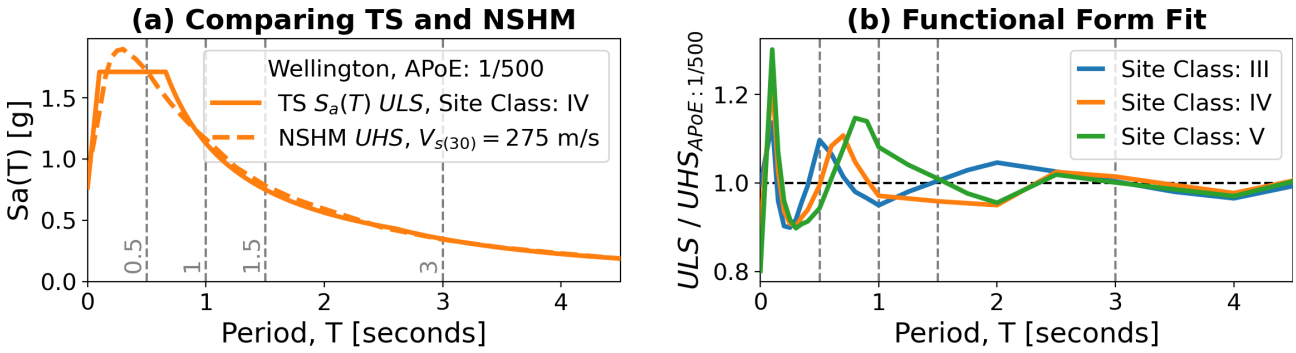

Figure 7: The functional form of the TS $S_a(T)$ spectrum for the Importance Level 2 (IL2) Ultimate Limit State, ULS, with respect to the National Seismic Hazard Model (NSHM) uniform hazard spectrum, UHS. (a) The TS's ULS for Wellington, Site Class IV (solid) and the NSHM UHS for $V_{s(30)} = 275$ m/s (dashed). (b) The ratio of the TS's ULS functional form to the NSHM's UHS, for Site Classes III, IV, and V (blue, orange, green respectively).

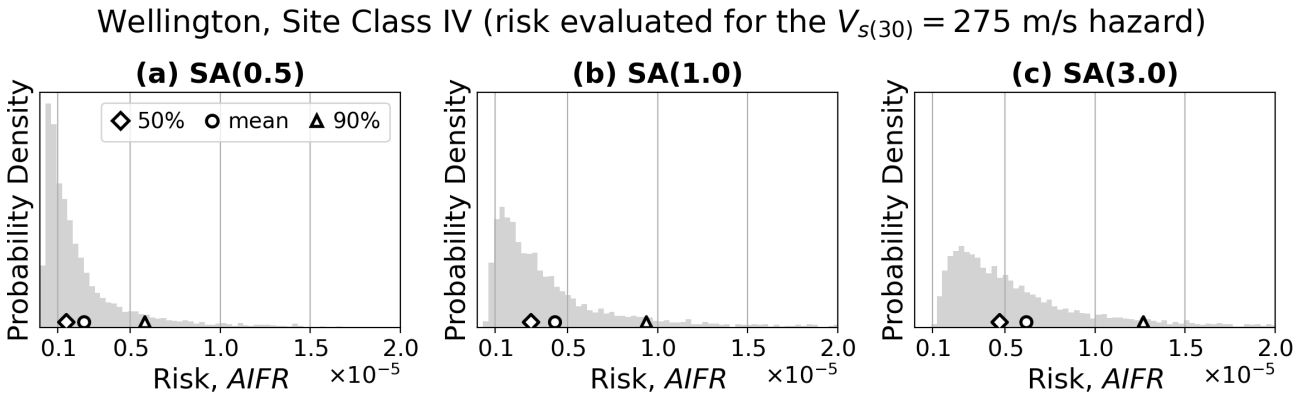

Figure 8: Risk distributions over the suite of fragilities (Fig 6), where TS Site Class IV with an annual probability of exceedance of 1/500 is the ultimate limit state (ULS) for a Wellington site with $V_{s(30)} = 275$ m/s (Fig 7a). (a) The gray histogram shows the distribution of risk for a period of T = 0.5 seconds, with the 50th percentile, mean, and 90th percentiles marked by a diamond, circle, and triangle, respectively. (b) Period of T = 1 seconds. (c) Period of T = 3 seconds.

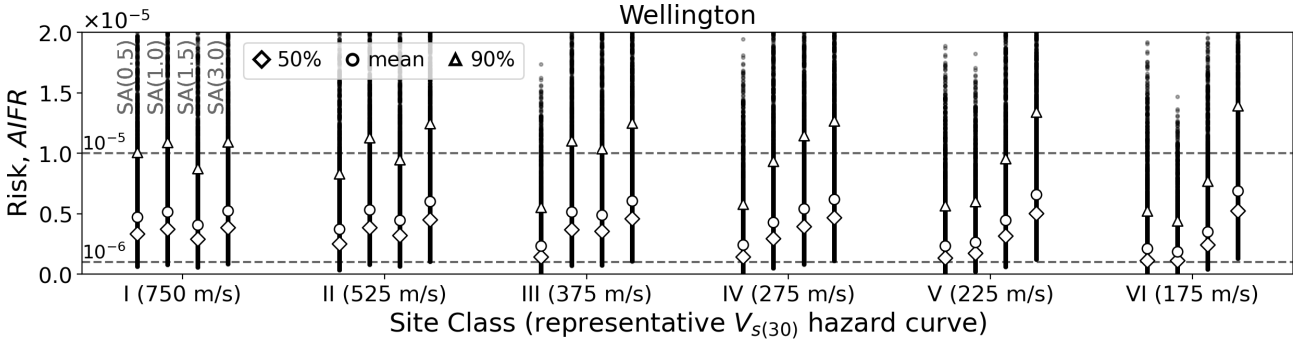

Figure 9: Risk distributions for Wellington. Each vertical line corresponds to one histogram as shown in Fig. 8, where the ultimate limit state (ULS) is defined by the Site Class (shown in groups) and the risk assessment uses the $V_{s(30)}$ corresponding to the site class's representative hazard curve. Each Site Class grouping shows the risk distribution for the fundamental periods T = 0.5, 1, 1.5, and 3 seconds (left to right). The 50th percentile, mean, and 90th percentile are marked by a diamond, circle, and triangle, respectively. The horizontal dashed lines mark $AIFR = 10^{-6}$ and 10^{-5}.

variability is explored in Figure 10, using a single fragility with $CMR = 6$ and $\beta = 0.45$. The trends revealed in this study are indicative of the shifts that would also occur in the full risk distributions.. The x-axis is decreasing values of $V_{s(30)}$, with dotted vertical lines showing the boundaries between each site class. Each site class's label is located at its representative $V_{s(30)}$ value. Above these labels are solid markers for the risk of three periods (blue, orange, and green for $T = 0.5$, 1, and 3 seconds), showing the fatality risk for the site class's *IL2 ULS* design spectrum, evaluated at the representative $V_{s(30)}$ hazard curve. However, a site may have a different $V_{s(30)}$ value while still falling in the same site class, resulting in a different underlying hazard curve. The effect of this hazard change on the risk is depicted in the lines extending in both directions from each solid marker. In most cases, the risk increases as the soil softens ($V_{s(30)}$ decreases). This increase continues until it hits the discontinuity at the site class boundary, when the $V_{s(30)}$ is assigned to the higher site class.

The peak in risk near each site class's softer boundary (lower

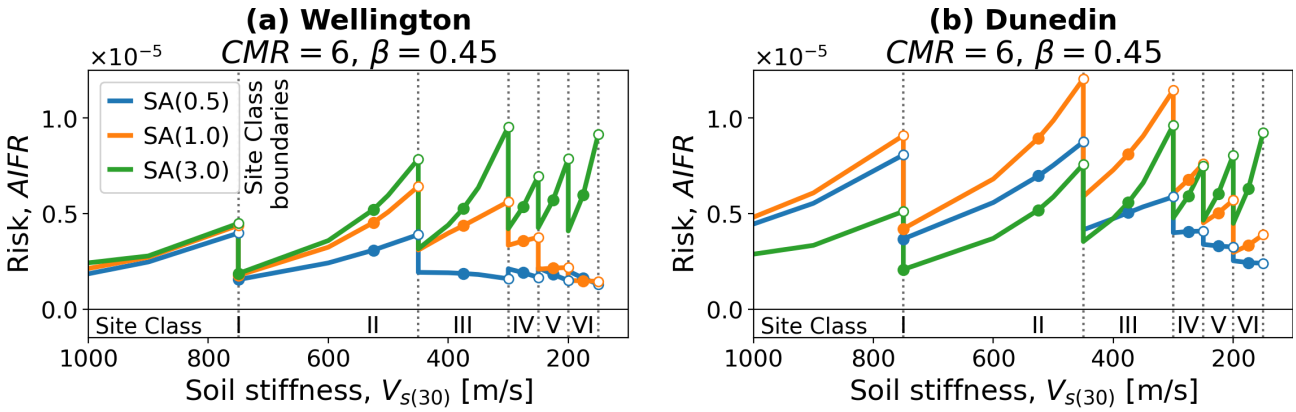

Figure 10: Impact of soil stiffness on risk, assuming a collapse fragility with CMR = 6, β = 0.45 for (a) Wellington and (b) Dunedin. The ultimate limit state (ULS) is defined by the TS Site Class (separated by vertical lines, the location of the label marks the site class's representative $V_{s(30)}$ value). The risk is shown for the fundamental periods T = 0.5, 1, and 3 seconds (blue, orange, green, respectively). The solid circle marker above each site class label is the risk for the representative $V_{s(30)}$ value. The open circles show the discontinuity between site classes, where the boundary $V_{s(30)}$ value is assigned to the higher site class. Note that this assumes perfect knowledge of the $V_{s(30)}$ value, whereas the TS assigns uncertainty bounds for conservatism around the site class boundaries.

$V_{s(30)}$) deserves further consideration. These peaks are mitigated by the TS's requirements for determining a site's $V_{s(30)}$ value. Rather than assuming precise knowledge of $V_{s(30)}$, the TS specifies a level of uncertainty ranging from 5-30%, depending on the method used for evaluating the V_s profile [5]. This means that any $V_{s(30)}$ within a boundary's uncertainty window will be assigned both site classes, with the *ULS* design spectrum taken as the envelope of both. Functionally, this pushes the discontinuity away from the site class boundary in the direction of the higher risk, reducing the height of the peak.

While the $V_{s(30)}$ trends in Figure 10 are similar between Wellington and Dunedin (subfigures a and b), the amplitudes are different. So far period and site stiffness are the main variables that have been considered for their influence on risk. The next section will consider the variability among locations across New Zealand.

Multiple Locations

Just as period and soil stiffness affect the shape of the hazard curve, and therefore the risk, so does location. Figure 11a shows hazard curves for four locations, considering $T = 1$ second, $V_{s(30)} = 275$ *m/s* and normalised based on the hazard at an *APoE* of 1/500. The normalised hazard curves for Christchurch and Wellington (orange and red) are nearly identical, resulting in very similar risk distributions (compare Figures 8b and Figure 12b).

Auckland and Dunedin (blue and green) also have similar normalised hazard curves, with relatively higher probabilities for high intensities. These shapes alone would result in higher risk for both cities, as compared to Wellington and Christchurch. However, as can be seen in Figure 11b, the TS proposed *ULS* design spectrum for Auckland is over 30% higher than the $UHS_{APoE:1/500}$, due to the lower bound hazard defined as the 90^{th} percentile of Auckland's hazard [3]. The impact of this lower bound is displayed in Figure 12a, where Auckland's risk distribution is lower than that of Christchurch (12b) and over 50% lower than Dunedin's (12c), despite the similar shape of the hazard curve.

The fact that Dunedin's risk is higher than that of Wellington and Christchurch is driven by the hazard being dominated by a nearby fault with low probability of occurrence, which increases the lower probabilities of exceedance with respect to the *APoE* of 1/500. This suggests again that, if uniform risk throughout the country were a primary objective, some adjustment could be applied to the *ULS* spectra in locations such as Dunedin. However, as with the previously mentioned period-based variability, the SRWG decided that the additional complexity of a location-specific adjustment was not warranted.

Finally, the results are expanded to consider a set of twelve locations. As before when comparing results across multiple variables, the histograms from Figure 12 are reoriented as vertical lines, with the white markers denoting the summary metrics of each distribution. Here, the figure shows results for Site Class IV, with each grouping representing one of the twelve locations and four periods for each. Once again, longer periods tend to have higher risk, though both the strength of that trend and the total risk depends on the location. While it is informative to display the risk distributions in this way, the increased number of hazard parameters make it difficult to identify trends. To that end, the results are reconfigured in Figure 14 to compare trends in the mean across the three hazard parameters: period, site class, and location. The mean risk is within the 10^{-6} to 10^{-5} tolerability range for all hazard combinations (shown in gray). The variability in the mean risk is most clear between locations, with the lowest risk for Christchurch and Queenstown versus the highest risk for Dunedin, Gisborne, and Napier. While this variability is due to the changing shape of the hazard curve, it is difficult to visualise or make sense of this effect, given the complex spatial distribution of faults and the rates of rupture on those faults. (Recall that the particularly low risk for Auckland is due to the adjustment for the lower bound hazard, rather than to the shape of the hazard curve.)

The scalar nature of period and site class (soil stiffness) makes it easier to characterise the effect of those parameters on the shape of the hazard curve. Yet the comparisons on the right half of Figure 14 does not reveal strict trends across these parameters. The previously observed trend of higher risk for longer periods is disrupted by the increased variability in $T = 0.5$ and 1 seconds. Similarly, there appears to be a decrease in risk as the site class increases from I to III but then the trend is disrupted by increased variability. These trends are explored further in Figure 15, which disaggregates the period groupings by site class. For $T = 0.5$, there is a clear decrease in risk as the site class increases from I to VI. This trend gradually fades as the period lengthens, until $T = 3$

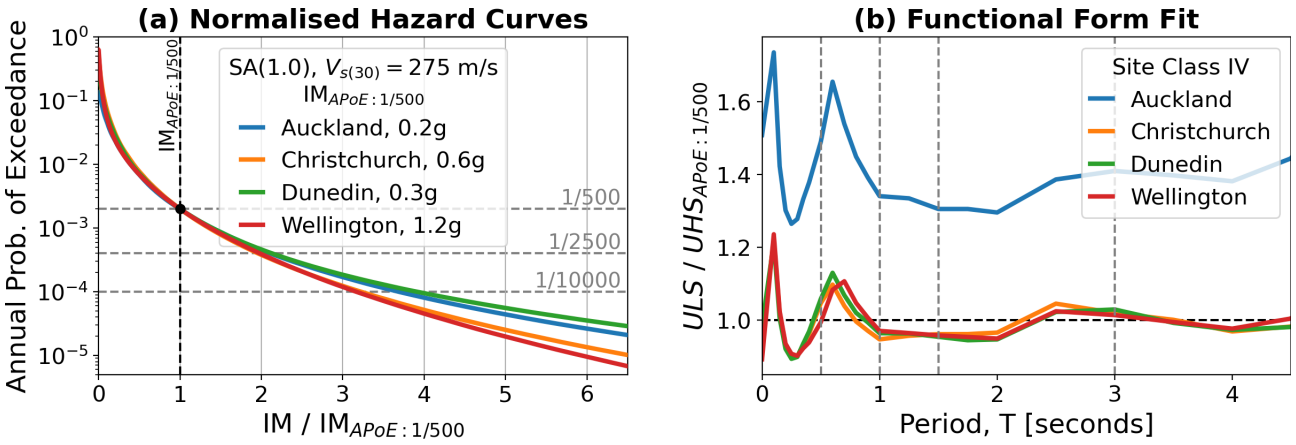

Figure 11: Hazard curves and their relation to the ULS value, per location. (a) The slope of the hazard curves for four locations, normalized by the values listed in the legend for the shaking intensity with a 1/500 annual probability of exceedance, $IM_{APoE:1/500}$. The hazard curves are for the fundamental period T = 1 second and $V_{s(30)} = 275$ m/s. (b) The ratio of the TS's ULS functional form to the NSHM's UHS for four locations.

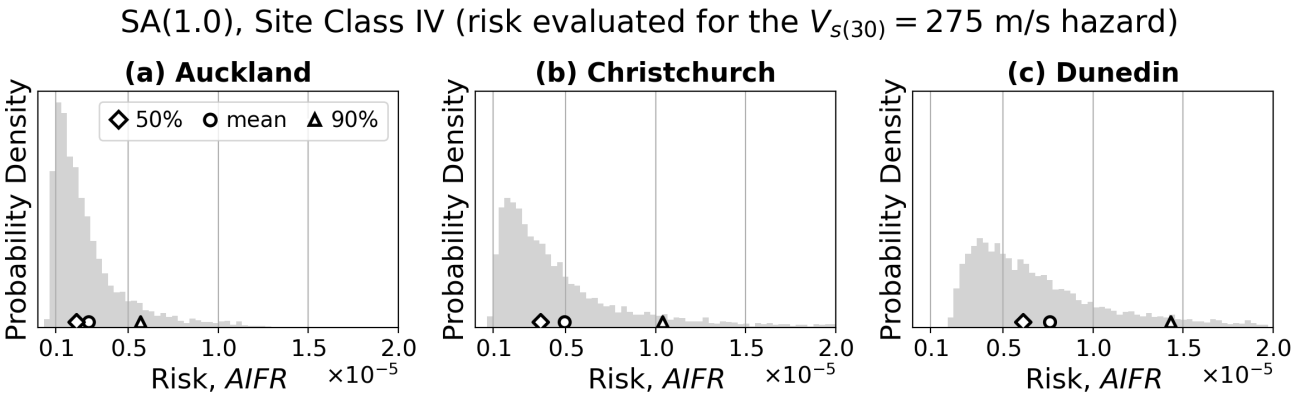

Figure 12: Risk distributions by location, where TS Site Class IV is the ultimate limit state (ULS), assessed using the hazard curve for a fundamental period of T = 1 second and $V_{s(30)} = 275$ m/s. (a) The gray histogram shows the distribution of risk for Auckland, with the 50th percentile, mean, and 90th percentiles marked by a diamond, circle, and triangle, respectively. (b) Christchurch. (c) Dunedin. (Note that Fig 8b is the equivalent figure for Wellington.)

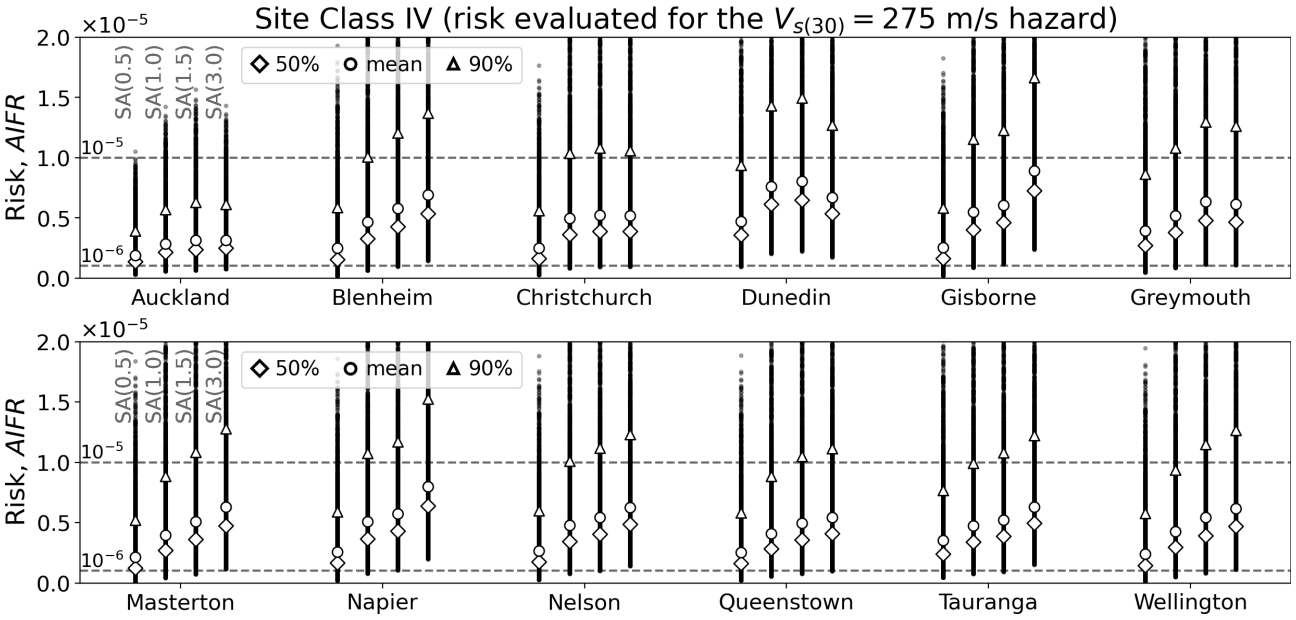

Figure 13: Risk distributions grouped by location, where the ultimate limit state (ULS) is defined by Site Class IV and the risk is evaluated for the $V_{s(30)} = 275$ m/s hazard curve. Each vertical line corresponds to one histogram as shown in Fig. 12. Each location grouping shows the risk distribution for the periods T = 0.5, 1, 1.5, and 3 seconds (left to right). The 50th percentile, mean, and 90th percentile are marked by a diamond, circle, and triangle, respectively. The horizontal dashed lines mark AIFR = 10^{-6} and 10^{-5}.

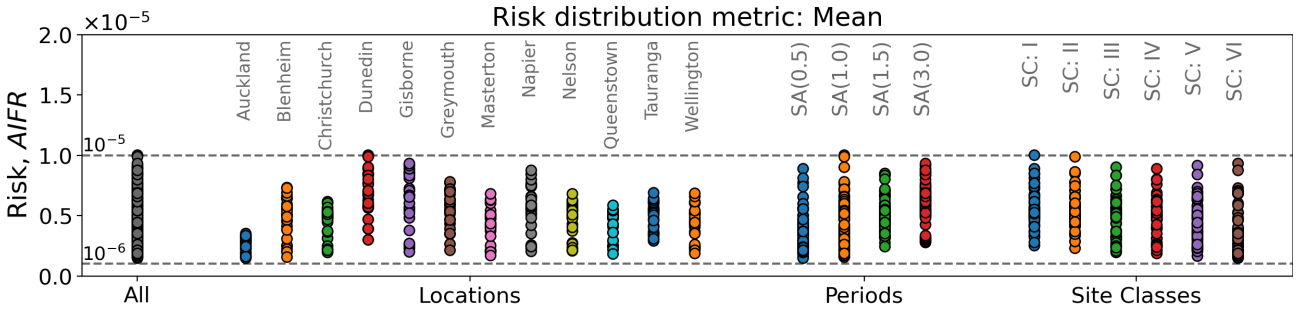

Figure 14: The mean values of each risk distribution across all hazard parameters (on the left, in gray). The three groups show the trends across four periods, six site classes, and twelve locations. The horizontal dashed lines mark AIFR = 10^{-6} ***and*** 10^{-5}***.***

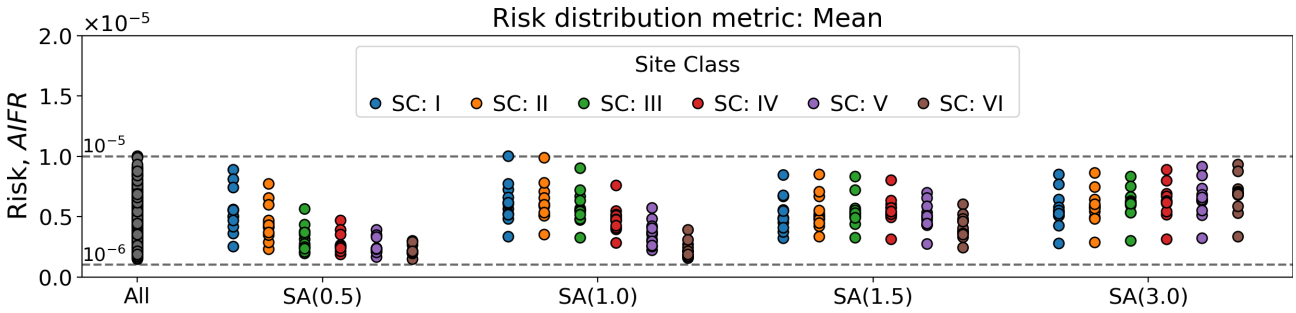

Figure 15: The mean values of each risk distribution across all hazard parameters (on the left, in gray). The four groups show increasing periods, left to right, and are disaggregated by site class. The horizontal dashed lines mark AIFR = 10^{-6} ***and*** 10^{-5}***.***

seconds shows a slight increase in risk as the site class increases. Looking instead at each period group's Site Class IV, V, and VI results (red, purple and brown, respectively) the risk increases with period as previously noted. These patterns help resolve the ambiguity in Figure 14's results for period and site class: the site class dominates the risk variability for shorter periods, obscuring the trend that is more apparent at longer periods. Conversely, the period dominates the risk variability for higher site classes. Once again, while these effects could be controlled by introducing risk factors, the SRWG chose to accept this variability in risk for the sake of simplicity.

Despite the variability among the results, the means remain within the tolerability range. Equivalent figures would show that the 90^{th} percentile results are all less than $2x10^{-5}$. In fact, the 90^{th} percentile is typically below $1.5x10^{-5}$, with the exception of Dunedin, Gisborne, and Napier for some combinations of site classes and periods. Recalling the criteria for tolerability, wherein the majority of the of risk distribution should fall in the low end of the 10^{-6} to 10^{-5} tolerability range and the 90^{th} is ideally no more than $2x10^{-5}$, these results suggest that the *APoE* of 1/500 is appropriate for *ULS* in IL2 buildings. The fact that the upper tail of the distribution extends beyond 10^{-5} can be tolerated both in light of the "blurred" definition of the risk tolerability range and the fact that fatality risk is only one of many drivers in the SRWG's process. It is risk-informed rather than risk-targeted, as seen by the development process of starting with a *ULS* design spectrum derived from other constraints, then checking whether it results in tolerable risk. Thus, based on these results, the SRWG confirmed that the *APoE* of 1/500 was an appropriate selection for the IL2 *ULS*.

COMPARISON WITH NZS 1170.5:2004

The previous section discussed the formal life-safety risk assessment for the SRWG decision making process, considering the TS *ULS* design spectrum as the input design requirements. However, the methodology can be used for any potential *ULS* spectrum. To that end, this section compares the risk associated with the proposed TS against that from the NZS 1170.5:2004.

First, it is useful to see how the spectra compare, as shown in Figure 16. This type of comparison requires a simplifying assumption for equivalent NZS and TS site classes, as there is no direct correlation between NZS site classes and $V_{s(30)}$ values. Rather than apply a rigorous comparison across all possible combinations, the lefthand panels in Figure 16 compare NZS Site Class C with TS Site Class III, which is a likely outcome for a $V_{s(30)}$ of 375 *m/s*. Similarly, the righthand panels compare NZS Site Class D with TS Site Class IV, for a $V_{s(30)}$ of 275 *m/s*.

The dashed black line in each subfigure represents the NZS 1170.5:2004 IL2 *ULS* design spectrum. These spectra were defined based on a previous NSHM, such that they are typically not consistent with the current NSHM or the proposed TS spectra. By comparing the black spectrum with the colors representing multiple *APoE* spectra from the TS, an "equivalent *APoE*" can be inferred for the NZS spectrum. For example, the black spectrum for Auckland $V_{s(30)} = 275$ *m/s* is close to 1/500 for periods above 1 second. Similarly, Wellington $V_{s(30)} = 275$ *m/s* is close to 1/250, whereas for $V_{s(30)} = 375$ m/s, the equivalent APoE is almost 1/100 for periods around 0.5 second. The implication of these figures is that anywhere the equivalent *APoE* for the NZS *ULS* is less than 1/500, the proposed TS *ULS* design spectra will reduce the life-safety risk, relative to that provided by NZS 1170.5:2004. Comparing the right and left panels in Figure 16 indicates that the equivalent *APoE* for Site Class C/III tends to be higher than that for Site Class D/IV. This is in part due to conservatism built into the selection of the Site Class D spectrum in the development of NZS 1170.5:2004 [3].

The risk mitigation effect of the proposed TS spectra for *ULS* can be seen in Figure 17. As indicated previously, $CMR = 6$ and $\beta = 0.45$ are used as an informal "average" fragility to provide a rough estimate of the mean risk, as well as a reference

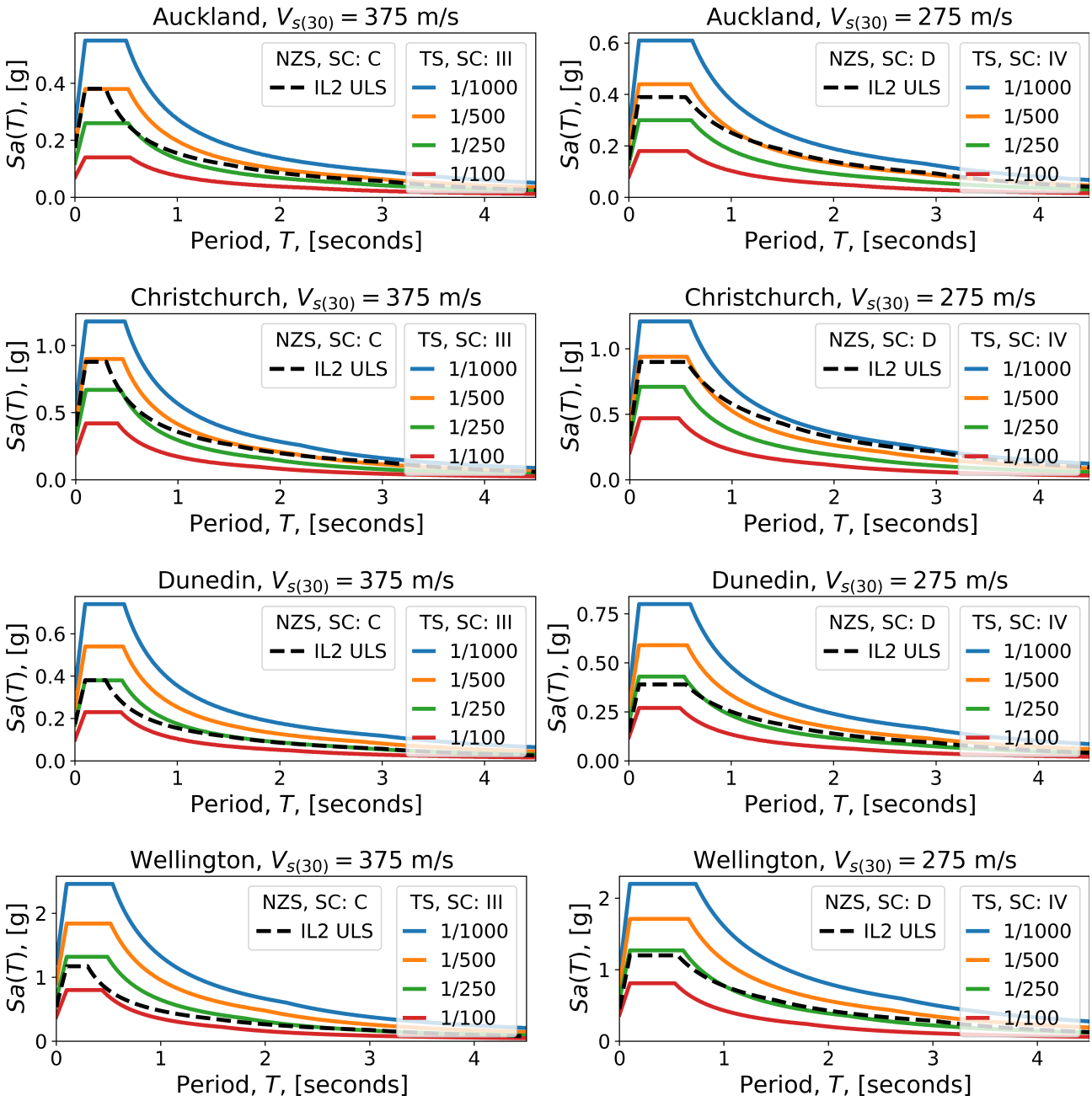

Figure 16: Comparisons between the NZS 1170.5:2004 spectra for an APoE of 1/500 (black) and a range of TS APoEs (1/100 through 1/1000, in color). Each row is a different location. The left and righthand panels are for $V_{s(30)} = 375$ and 275 m/s, respectively.

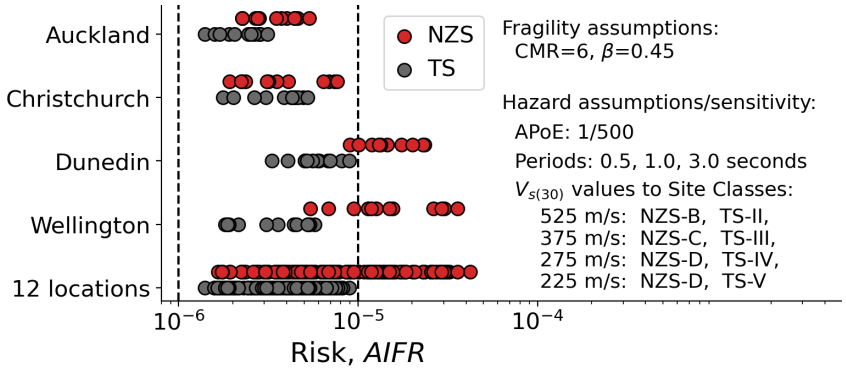

Figure 17: Comparing fatality risk for the TS versus NZS 1170.5:2004. All annual individual fatality risk (AIFR) values are calculated for a fragility with $CMR = 6$ and $\beta = 0.45$. Each point represents one pairing of location, period, and site stiffness, as outlined in the figure.

for the relative positions of the full risk distributions. Each circle represents one set of hazard parameters: a combination of location, period (T = 0.5, 1, and 3 seconds), and $V_{s(30)}$ (525, 375, 275, and 225 *m/s*). As in Figure 16, simplifying assumptions are needed to compare the NZS and TS site classes for each $V_{s(30)}$. These assumptions are provided in Figure 17 for each of the $V_{s(30)}$ values. Again, these do not constitute a rigorous comparison, due to the loose link between NZS1170.5:2004 site classes and $V_{s(30)}$ values.

The x-axis in Figure 17 shows the fatality risk, *AIFR*. The red markers show the risk associated with the *ULS* spectra for the existing NZS1170.5:2004 (NZS), while the gray markers show the same for the TS. The bottom row, which includes all twelve locations, shows that the risk for the NZS is centered around $1x10^{-5}$. The upper rows for individual locations reveal that the risk for Dunedin and Wellington falls mostly above $1x10^{-5}$, which the risk for Auckland and Christchurch falls below $1x10^{-5}$. This is in contrast with the results for the TS, in which all the gray markers fall below $1x10^{-5}$. While Dunedin still has higher risk than the other three locations, there is less variability in the risk for the TS, considering location, period, and site class. This move towards more uniform risk is again consistent with the intent of the risk-informed approach.

LIFE-SAFETY RISK FOR IMPORTANCE LEVEL 3

It is also of interest to assess the life-safety risk for Importance Level 3 buildings. This category includes, among other things, large buildings with more than 5000 occupants. The *APoE* for IL3 buildings is 1/1000, as per AS/NZS 1170.0. The following discussion considers the implications of this shift in *APoE* on the fatality risk, *AIFR*.

Recall that *AIFR* is the "annual individual fatality risk." This *AIFR* is the risk to each individual in the building and does not consider the collective risk to the the occupants as a whole. While this is a valuable and commonly used metric in risk analysis, it cannot address societal aversion to mass casualty events. For this purpose, many sectors, including dam safety, use *F-N* curves to define risk limits on *N* number of fatalities, where one death is more tolerable than one hundred, which is more tolerable than one thousand, etc. [12] The implication is that it is also less tolerable for an IL3 building with 5000 occupants to collapse than a smaller building with 50 occupants.

This aversion to large building collapses is managed through stricter design limits, such as an *APoE* of 1/1000 instead of 1/500. Functionally, this is equivalent to a lower *AIFR* tolerability. In fact, *F-N* curve limits can be reframed as adjustments to an *AIFR* limit, resulting in *ULS* scale factors that increase with occupancy, not just a single step change at 5000 occupants [9]. The TS approach, however, maintains consistency with both the IL2 approach and AS/NZS 1170.0 by simply specifying a single *APoE* for IL3. Figure 18 shows significant shifts in the IL2 to IL3 *AIFR* risk distributions for each of twelve locations, assuming $T = 1$ second and Site Class IV. For the IL3's *APoE* of 1/1000, the 90^{th} percentile risk is typically below $0.5x10^{-5}$, while the mean is typically around $2x10^{-6}$. This is roughly half of the *AIFR* risk for the IL2's *APoE* of 1/500.

CONCLUSIONS

This paper has demonstrated the life-safety risk assessment methodology used by the Seismic Risk Working Group (SRWG) to consider the tolerability of risk. To that end, it focused on the fatality risk associated with using the proposed TS to define the acceleration spectra for the ultimate limit state, ULS, in the design of Importance Level 2 buildings. The ULS checks for IL2 buildings are based on a design intensity with an annual probability of exceedance, *APoE*, of 1/500.

The risk tolerability is based on the annual individual fatality risk, *AIFR*. While there is no local or global consensus on what *AIFR* values are tolerable for new building design, there are precedents that suggest a range of 10^{-6} to 10^{-5} may be appropriate. The use of a range is also consistent with the SRWG's approach of assessing a risk distribution across all code-conforming buildings, rather than considering a single value. Therefore, the SRWG selected a risk tolerability range of 10^{-6} to 10^{-5}, in which the risk for the majority of buildings should fall in the lower end of the risk range and the 90^{th} percentile is ideally no more than $2x10^{-5}$.

The risk assessment methodology is made up of four modules, which characterize the shaking hazard, building collapse performance, the probability of fatality given collapse, and the variety among buildings. Inputing a proposed design spectrum, $S_a(T)$, into the methodology results in a distribution of fatality risk associated with that spectrum. Each *AIFR* value in the distribution represents one building's collapse fragility, paired with a hazard curve from the 2022 National Seismic Hazard Model (NSHM) to produce a fatality risk accumulated over the full range of shaking intensities. Together, the distribution of individual *AIFR* values represents the expected range of fatality risk among all the potential buildings that could be designed in conformance with minimum design requirements.

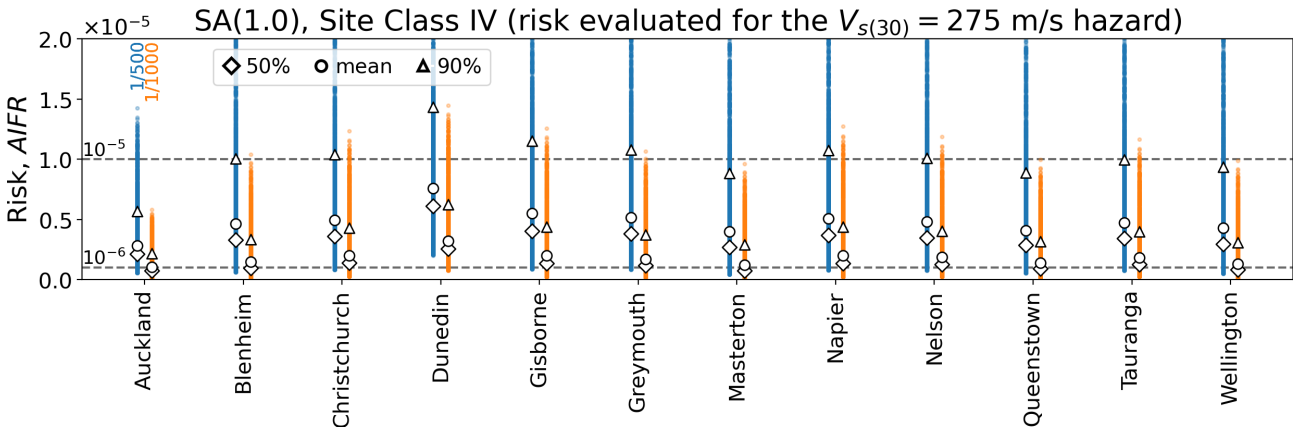

Figure 18: Risk distributions by location, considering ULS with APoEs of 1/500 and 1/1000 for Importance Levels 2 and 3. The vertical risk distributions are marked with a diamond, circle, and triangle for the 50^{th} percentile, mean, and 90^{th} percentile.

The results show that the risk distributions for a *ULS* with an *APoE* of 1/500 do indeed fall within the SRWG's criteria for tolerable risk. However, there are two dimensions in which the risk is variable. The variability among potential designs for a single location, site class, and period has already been mentioned as a fundamental characteristic of the SRWG risk methodology. The risk is also variable across those three hazard parameters, as the whole distribution maybe increased or decreased depending on the relationship between the *ULS* value and the hazard curve. For example, the shape of the hazard curve for longer periods tends to result in more risk. The shape of the hazard curve also depends on location such that, for example, Dunedin has higher risk than Wellington. While this effect could be controlled formally by a risk factor varying with period or location, the SRWG determined that it was not worth the added complexity at this time. This is particularly true given the inherent variability that exists among buildings, regardless of the adjustments that came be implemented among hazard parameters.

There is one context in which the risk is systematically reduced through adjustments to *ULS*: sites in Auckland and Northland, where the lower bound hazard is applied. This increases the *ULS* design spectra with respect to the mean NSHM uniform hazard spectra, resulting in significantly reduced life-safety risk with Auckland's 90^{th} percentile risk on the order of the mean risk for other locations.

The life-safety risk for the proposed TS can also be compared with the risk associated with the *ULS* requirements in NZS1170.5:2004. A simple comparison between the two sets of *ULS* spectra shows that the NZS IL2 *ULS* design spectrum is no longer consistent with an *APoE* of 1/500 from the updated NSHM. In some cases (Auckland and Christchurch), the *ULS* is similar to an *APoE* of 1/500, while in others it may be as high as 1/100 but typically closer to 1/250. Comparing the *AIFR* risk for the two cases suggests that the proposed TS provides more uniform (and lower) risk across the country.

Finally, the life-safety risk for high occupancy buildings (IL3) is compared with that of IL2. Shifting from an *APoE* of 1/500 to 1/1000 functionally reduces the *AIFR*, which is a metric for individuals. The concern for mass casualties in the larger building requires a different risk metric for increasing numbers of fatalities. Rather than explicitly quantifying this metric for collective risk, the TS implicitly accounts for it by reducing the *APoE*, and hence, the *AIFR* in high occupancy buildings. The shift from an *APoE* of 1/500 to 1/1000 results in roughly half the *AIFR* risk.

The SRWG's life-safety risk assessment methodology provides a way of calculating not just the expected risk but estimates the full range of risk, acknowledging variability among buildings that may be designed in conformance with minimum design requirements. This range allows decision makers to better assess the implications of changes to the design spectra. Based on the risk results presented here, the SRWG determined that an *APoE* of 1/500 was a tolerable choice for the IL2 *ULS* spectra.

ACKNOWLEDGMENTS

The authors acknowledge the contributions and insight of the other members of the Seismic Risk Working Group, as well as John Hooper. This work was supported by Engineering New Zealand (ENZ) and by the Ministry for Business, Innovation, and Employment (MBIE).

REFERENCES

1 Gerstenberger MC, Bora S, Bradley BA, DiCaprio C, Kaiser A, Manea EF, Nicol A, Rollins C, Stirling MW, Thingbaijam KKS, Dissen RJV, Abbott ER, Atkinson GM, Chamberlain C, Christophersen A, Clark K, Coffey GL, de la Torre CA, Ellis SM, Fraser J, Graham K, Griffin J, Hamling IJ, Hill MP, Howell A, Hulsey AM, Hutchinson J, Iturrieta P, Johnson KM, Jurgens VO, Kirkman R, Langridge RM, Lee RL, Litchfield NJ, Maurer J, Milner KR, Rastin S, Rattenbury MS, Rhoades DA, Ristau J, Schorlemmer D, Seebeck H, Shaw BE, Stafford PJ, Stolte AC, Townend J, Villamor P, Wallace LM, Weatherill G, Williams CA and Wotherspoon LM (2023). "The 2022 Aotearoa New Zealand National Seismic Hazard Model: Process, Overview, and Results". *Bulletin of the Seismological Society of America*: 7–36. https://doi.org/10.1785/0120230182

2 Standards New Zealand (2004). *NZS 1170.0:2004 Structural Design Actions Part 5: Earthquake Actions - New Zealand*. www.standards.govt.nz

3 Elwood K and Dhakal R (2025). "Background to proposed changes to NZS 1170.5:2004". *Bulletin of the New Zealand Society for Earthquake Engineering*, **58**(1): i–ii. https://doi.org/10.5459/bnzsee.1734

4 Francis T, Sullivan T, Hulsey AM and Elwood KJ (2025). "Recommendations for the shape of the design response spectrum in the New Zealand seismic loadings technical specification". *Bulletin of the New Zealand Society for Earthquake Engineering*, **58**(2): 83–97. https://doi.org/10.5459/bnzsee.1692

5 Lee R, Cubrinovski M and Bradley B (2025). "Site classification methodology for TS 1170.5 design spectra". *Bulletin of the New Zealand Society for Earthquake Engineering*, **58**(1): 11–39. https://doi.org/10.5459/bnzsee.1686

6 New Zealand Government (1992). "The New Zealand Building Code". https://www.legislation.govt.nz/regulation/public/1992/0150/latest/DLM162576.html

7 Luco N, Ellingwood BR, Hamburger RO, Hooper JD, Kimball JK and Kircher CA (2007). "Risk-Targeted versus Current Seismic Design Maps for the Conterminous United States". *Structural Engineering Association of California 2007 Convention Proceedings*: 1–13.

8 Silva V, Crowley H and Bazzurro P (2016). "Exploring risk-targeted hazard maps for Europe". *Earthquake Spectra*, **32**: 1165–1186. https://doi.org/10.1193/112514EQS198M

9 Horspool N, Hulsey AM, Elwood KJ and Gerstenberger MC (2023). "Risk-targeted hazard for seismic design in New Zealand considering individual and societal risk targets". *Earthquake Spectra*, **39**: 1007–1036. https://doi.org/10.1177/87552930231156947

10 Standards New Zealand (2002). *AS/NZS 1170.0:2002 Structural Design Actions Part 0: General Principles*. www.standards.govt.nz

11 EQC TTA (2023). *"Natural Hazard Risk Tolerance Literature Review"*. Technical report, Toka Tū Ake EQC. https://www.eqc.govt.nz/assets/Publications-Resources/Risk-Tolerance-Literature-Review.pdf

12 Jonkman SN, Gelder PHV and Vrijling JK (2003). "An overview of quantitative risk measures for loss of life and economic damage". *Journal of Hazardous Materials*, **A99**: 1–30. https://doi.org/10.1016/S0304-3894(02)00283-2

13 Clarke LB, Kelly SD, FitzGerald T, Pondard N and Wilson-Rooy M (2021). *"Stocktake of Existing Risk Tolerance*

Frameworks". Technical report, GNS Science Consultancy Report 2021/71.

14 ISO 2394:2015 (2015). *"General Principles on Reliability for Structures"*. Technical report, International Organization for Standardization (ISO),.

15 Douglas J, Ulrich T and Negulescu C (2013). "Risk-targeted seismic design maps for mainland France". *Natural Hazards*, **65**: 1999–2013. https://doi.org/10.1007/s11069-012-0460-6

16 Baker JW, Bradley B and Stafford P (2021). *Seismic Hazard and Risk Analysis*. Cambridge University Press, ISBN 9781108348157. https://doi.org/10.1017/9781108425056

17 FEMA P695 (2009). *"Quantification of Building Seismic Performance Factors"*. Technical report, Applied Technology Council. www.ATCouncil.org

18 Eads L, Miranda E and Lignos DG (2015). "Average spectral acceleration as an intensity measure for collapse risk assessment". *Earthquake Engineering & Structural Dynamics*, **44**: 2057–2073. https://doi.org/10.1002/eqe.2575

19 Eads L, Miranda E and Lignos D (2016). "Spectral shape metrics and structural collapse potential". *Earthquake Engineering & Structural Dynamics*, **45**: 1643–1659. https://doi.org/10.1002/eqe.2739

20 Zhong K, Chandramohan R, Baker JW and Deierlein GG (2022). "Site-specific adjustment framework for incremental dynamic analysis (SAF-IDA)". *Earthquake Spectra*, **38**: 1893–1917. https://doi.org/10.1177/87552930221083688

21 Bradley BA (2010). "A generalized conditional intensity measure approach and holistic ground-motion selection". *Earthquake Engineering & Structural Dynamics*, **40**. https://doi.org/10.1002/eqe.995

22 FEMA P-58 (2012). *"Seismic Performance Assessment of Buildings: Volume 1 (Methodology)"*. Technical report, Applied Technology Council.

23 Zareian F and Krawinkler H (2007). "Assessment of probability of collapse and design for collapse safety". *Earthquake Engineering & Structural Dynamics*, **36**: 1901–1914. https://doi.org/10.1002/eqe.702

24 Horspool N, Elwood KJ, Johnston D, Deely J and Ardagh M (2020). "Factors influencing casualty risk in the 14th November 2016 MW7.8 Kaikōura, New Zealand earthquake". *International Journal of Disaster Risk Reduction*, **51**. https://doi.org/10.1016/J.IJDRR.2020.101917

25 Horspool N (2022). *"Life-safety risk in earthquakes: Investigating risk factors and development of risk management tools"*. Ph.D. Thesis, The University of Auckland, New Zealand. https://hdl.handle.net/2292/62613

26 FEMA (2001). *"HAZUS MH-2.1 Advanced Engineering Building Module (AEBM)"*. Technical report, Federal Emergency Management Agency, Mitigation Division.

27 Zaidi F, Elwood KJ and Hulsey AM (2024). "A Framework For Incorporating Fatality Risk In Seismic Assessment Methodology In New Zealand". *18th World Conference on Earthquake Engineering*.

28 FEMA (2012). *"Hazus Multi-hazard Loss Estimation Methodology, Earthquake Model, Hazus-MH 2.1 Technical Manual"*. Technical report, Federal Emergency Management Agency, Mitigation Division.

29 So E (2016). *Estimating Fatality Rates for Earthquake Loss Models*. Springer, ISBN 978-3-319-26837-8, 71 pp.

30 Yeow TZ, Orumiyehei A, Sullivan TJ, MacRae GA, Clifton GC and Elwood KJ (2018). "Seismic performance of steel friction connections considering direct-repair costs". *Bulletin of Earthquake Engineering*, **16**: 5963–5993. https://doi.org/10.1007/s10518-018-0421-x

31 John L, Williamson MB and Sullivan TJ (2023). "Investigating the Impact of Design Criteria on the Expected Seismic Losses of Multi-Storey Office Buildings". *Bulletin of the New Zealand Society for Earthquake Engineering*, **56**: 11–28. https://doi.org/10.5459/bnzsee.56.1.11-28

32 Orumiyehei A (2022). *"Probabilistic Displacement Based Seismic Assessment"*. Ph.D. Thesis, University of Canterbury, Christchurch, New Zealand.